UTBEST-3D – An adaptive Discontinuous Galerkin Solver for Three-Dimensional Shallow Water Equations

Vadym Aizinger[†] and Clint Dawson[†]

July 7, 2005

Abstract

UTBEST-3D is a simulator for 3D shallow water equations with a free surface that employs a local discontinuous Galerkin method. In our previous simulator, UTBEST, we implemented the local discontinuous Galerkin method for depth inegrated shallow water equations. UTBEST-3D is to a great degree compatible with input and output formats of UTBEST (and those of the ADCIRC simulator of Luettich et al [4]).

1 Introduction

UTBEST-3D was developed at the Center for Subsurface Modeling(CSM), University of Texas at Austin. The main purpose of this document is to present a brief description of the mathematical and numerical models implemented in UTBEST-3D as well as to give an overview of the main configuration options of the simulator and input files.

[†]Center for Subsurface Modeling - C0200; Institute for Computational Engineering and Sciences (ICES); The University of Texas at Austin; Austin, TX 78712. This research was supported by NSF grant DMS-0107247 and the Texas Water Development Board.

2 Mathematical Formulation

The mathematical model of three-dimensional constant density shallow water flow includes momentum equations for the horizontal velocity components, a continuity equation, and boundary and initial conditions. The domain over which these equations are defined has a free surface described by a kinematic boundary condition.

The conservative form of the momentum conservation equations can be written as follows:

$$\frac{\partial \mathbf{u}_{xy}}{\partial t} + \nabla \cdot \left(\mathbf{u}_{xy}\mathbf{u}^T - \mathcal{D}\nabla \mathbf{u}_{xy} \right) + g\nabla_{xy}\xi - f_c \mathbf{k} \times \mathbf{u}_{xy} = \mathbf{G}, \tag{1}$$

where $\nabla_{xy} = \left(\frac{\partial}{\partial x}, \frac{\partial}{\partial y}\right)$, ξ is the value of the z coordinate at the free surface, $\mathbf{u} = (u, v, w)^T$ is the velocity vector, $\mathbf{u}_{xy} = (u, v)^T$ is the vector of horizontal velocity components, f_c is the Coriolis coefficient, $\mathbf{k} = (0, 0, 1)$ a unit vertical vector, g is acceleration due to gravity, $\mathbf{G} = (G_x, G_y)$ is a vector of body forces (it can include atmospheric pressure terms, tidal forcing, etc.), and $\mathcal{D}$ is a tensor of eddy viscosity coefficients defined as follows:

$$\mathcal{D} = \begin{pmatrix} D_u & 0 \\ 0 & D_v \end{pmatrix} \tag{2}$$

with D_u, D_v being 3x3 symmetric positive-definite matrices.

The continuity equation can be written as

$$\frac{\partial u}{\partial x} + \frac{\partial v}{\partial y} + \frac{\partial w}{\partial z} = 0. \tag{3}$$

We augment the system with the following boundary conditions:

- At the bottom, we have no normal flow

  $$\mathbf{u}(z_b) \cdot \mathbf{n} = 0 \tag{4}$$

  and no slip for horizontal velocity components

  $$u(z_b) = v(z_b) = 0. \tag{5}$$

  where z_b is the value of the z coordinate at the sea bed and $\mathbf{n} = (n_x, n_y, n_z)^T$ is an exterior unit normal to the face.

- The free surface boundary conditions have the form:

$$\frac{\partial \xi}{\partial t} + u(\xi)\frac{\partial \xi}{\partial x} + v(\xi)\frac{\partial \xi}{\partial y} - w(\xi) = 0. \tag{6}$$

$$\frac{\partial u}{\partial \mathbf{n}} = \frac{\partial v}{\partial \mathbf{n}} = 0. \tag{7}$$

On the lateral boundaries, we can have several types of boundary conditions (note, that we assume all lateral boundaries to be strictly vertical; therefore, if $\mathbf{n} = (n_x, n_y, n_z)^T$ is an exterior normal to a lateral boundary face then $n_z = 0$):

- River boundary: Prescribed normal u_n and tangential u_τ velocities

$$un_x + vn_y = u_n, \qquad -un_y + vn_x = u_\tau, \tag{8}$$

  and prescribed surface elevation $\xi_r(x, y, t)$

$$\xi = \xi_r(x, y, t). \tag{9}$$

- Land boundary: No normal flow

$$u_n = \mathbf{u} \cdot \mathbf{n} = 0, \tag{10}$$

  and zero shear stress

$$\frac{\partial u_\tau}{\partial \mathbf{n}} = 0. \tag{11}$$

- Open sea boundary: Zero normal derivative of the horizontal velocity components

$$\frac{\partial u}{\partial \mathbf{n}} = \frac{\partial v}{\partial \mathbf{n}} = 0, \tag{12}$$

  and prescribed surface elevation $\xi_s(x, y, t)$

$$\xi = \xi_s(x, y, t). \tag{13}$$

- Radiation boundary: Zero normal derivative of the horizontal velocity components

$$\frac{\partial u}{\partial \mathbf{n}} = \frac{\partial v}{\partial \mathbf{n}} = 0. \tag{14}$$

Analytically, the free surface elevation can be computed using (6), but, numerically, a more robust way to do it is to integrate the continuity equation (3) over the depth and, taking into account the boundary conditions at the top and bottom, obtain the following 2D equation for the surface elevation commonly called the primitive continuity equation (PCE):

$$\frac{\partial \xi}{\partial t} + \frac{\partial}{\partial x}\int_{z_b}^{\xi} u dz + \frac{\partial}{\partial y}\int_{z_b}^{\xi} v dz = 0. \tag{15}$$

The equation above or, alternatively, the wave equation derived by substituting the 2D momentum equations in (15) is a standard part of just about every 2- and 3D shallow-water model in existence today, though using this equation to compute the position of the free surface within a framework of a 3D solver based on the discontinuous Galerkin method is not trivial, that is unless we resort to solving an auxiliary 2D problem as is done in many 3D shallow water solvers. We will discuss this issue in some detail in section 4.

Let us denote $h = \xi - z_b$. Then, we can rewrite conservation equations (15), (1) in the following compact form:

$$\frac{\partial h}{\partial t} + \nabla_{xy} \cdot \mathbf{C_H} = 0, \tag{16}$$

$$\frac{\partial \mathbf{u}_{xy}}{\partial t} + \nabla \cdot (\mathcal{C}_M - \mathcal{D}\nabla \mathbf{u}_{xy}) = \mathbf{F}, \tag{17}$$

where

$$\mathbf{C_H} = \begin{pmatrix} \int_{z_b}^{\xi} u\ dz \\ \int_{z_b}^{\xi} v\ dz \end{pmatrix},\ \mathcal{C}_M = \begin{pmatrix} u^2 + gh & uv \\ uv & v^2 + gh \\ uw & vw \end{pmatrix},\ \mathbf{F} = \begin{pmatrix} G_x + g\frac{\partial z_b}{\partial x} + f_c v \\ G_y + g\frac{\partial z_b}{\partial y} - f_c u \end{pmatrix}.$$

Thus, our system consists of the primitive continuity equation (16), two momentum conservation equations for horizontal velocity components (17), and the continuity equation (3).

3 General issues and solution strategy

3.1 Solution strategy

The general solution strategy employed in our implementation is not substantially different from ones found in other 3D solvers. The main differences lie in the fact that all state variables are approximated in space with functions which are continuous on each element but can be discontinuous

across inter-element boundaries. For time stepping, we use explicit Runge-Kutta methods, choosing the time step and scheme order appropriately to keep the error of the time stepping algorithm well within the error of space discretization.

Within a time step (substep in case of multistage Runge-Kutta methods), first, we solve the mass and momentum conservation equations. These equations are tightly coupled and must be dealt with simultaneously. Then, for given values of horizontal velocity components $\mathbf{u}_{xy} = (u, v)^T$, we compute vertical velocity w from the discrete continuity equation to obtain a divergence-free velocity field. The latter equation is not time-dependent and is solved as an initial value problem layer-by-layer starting at the bottom and using the solution from the layer below (or boundary condition (4) at the bottom in case of the bottommost layer) as an initial value.

Every few time steps the mesh geometry is updated using computed values of the surface elevation. Frequency of mesh update can be chosen according to the type of problem we are solving.

3.2 Computational mesh

The most common type of mesh employed in 3D finite element simulations of shallow-water flow is a 2D grid projected vertically and subdivided into layers using a Cartesian or σ-stretched coordinate system. This approach agrees well with the physical anisotropy of the problem, in which the vertically directed gravity force usually is the main body force acting on the system. The grids in our implementation also belong to this type. In our model, we use prismatic elements with triangular cross-section, strictly vertical lateral faces, and flat but not necessarily parallel top and bottom faces.

Since the surface elevation is one of the primary variables approximated in a discontinuous polynomial space, the grid determined by our discrete solution would also have a discontinuous free surface, thus, the lateral faces shared by neighboring elements in the uppermost layer of the mesh would, in general, not match. This causes the boundary integrals over those faces to be ill-defined. In order to avoid this problem, we smooth the free surface of our mesh (e.g., by the least squares fit) and compute all 3D integrals on a grid with a globally continuous free surface. This procedure only affects the geometry of elements and faces in the uppermost layer of the computational mesh and does not change in any way the computed values of the state variables or the discontinuous character of the numerical solution. Thus,

the local conservation properties of the Local Discontinuous Galerkin (LDG) method are not degraded by this mesh smoothing postprocessing. In our experiments, the stability and accuracy of the numerical solution did not seem to be significantly influenced by the mesh smoothing algorithm used.

4 Space Discretization, the LDG method

To discretize our problem in space using the LDG method, we first introduce an auxiliary flux variable $\mathcal{Q}$ and rewrite the momentum conservation equations in the mixed form:

$$\frac{\partial \mathbf{u}_{xy}}{\partial t} + \nabla \cdot (\mathcal{C}_M + \sqrt{\mathcal{D}}\mathcal{Q}) = \mathbf{F}, \tag{18}$$

$$\mathcal{Q} = -\sqrt{\mathcal{D}}\nabla \mathbf{u}_{xy}. \tag{19}$$

Let $\mathcal{T}_h$ be a general partition of our 3D domain Ω and let $\Omega_e \in \mathcal{T}_h$. To obtain a weak formulation we multiply the equations above by smooth test functions $\boldsymbol{\phi}$, Ψ; integrate them on each element $\Omega_e \in \mathcal{T}_h$; and, finally, integrate by parts obtaining the following expressions:

$$\int_{\Omega_e} \frac{\partial \mathbf{u}_{xy}}{\partial t}\ \boldsymbol{\phi}\ dxdydz + \int_{\partial\Omega_e} (\mathcal{C}_M + \sqrt{\mathcal{D}}\mathcal{Q}) \cdot \mathbf{n}\ \boldsymbol{\phi}\ ds \tag{20}$$

$$- \int_{\Omega_e} (\mathcal{C}_M + \sqrt{\mathcal{D}}\mathcal{Q}) \cdot \nabla \boldsymbol{\phi}\ dxdydz = \int_{\Omega_e} \mathbf{F}\ \boldsymbol{\phi}\ dxdydz,$$

$$\int_{\Omega_e} \sqrt{\mathcal{D}^{-1}}\ \mathcal{Q}\ \Psi\ dxdydz = -\int_{\partial\Omega_e} \mathbf{u}_{xy}\ \Psi \cdot \mathbf{n}\ ds \tag{21}$$

$$+ \int_{\Omega_e} \mathbf{u}_{xy}\ \nabla \cdot \Psi\ dxdydz, \tag{22}$$

where $\mathbf{n}$ is a unit exterior normal to Ω_e. This weak formulation is well defined for any $\mathbf{u}_{xy}(t,x,y,z) \in H^1(0,T;\ V^{d-1})$; $w(t,x,y,z) \in V,\ \forall t \in [0,T]$; $\boldsymbol{\phi}(x,y,z) \in V^{d-1}$; $\mathcal{Q}(t,x,y,z) \in Y^{d-1},\ \forall t \in [0,T]$; and $\Psi(x,y,z) \in Y^{d-1}$, where

$$V \stackrel{\text{def}}{=} L^2(\Omega) \bigcap \{u : u_{|\Omega_e} \in H^1(\Omega_e), \forall \Omega_e \in \mathcal{T}_h\}, \tag{23}$$

$$Y \stackrel{\text{def}}{=} L^2(\Omega)^d \bigcap \{\mathbf{q} : \mathbf{q}_{|\Omega_e} \in H^1(\Omega_e)^d, \forall \Omega_e \in \mathcal{T}_h\}. \tag{24}$$

Next, we seek to approximate $(\mathbf{u}_{xy}(t,\cdot), w(t,\cdot), \mathcal{Q}(t,\cdot))$, the solution to the weak problem, with a function $(\mathbf{U}_{xy}(t,\cdot), W(t,\cdot), \mathcal{Q}(t,\cdot)) \in U_h \times W_h \times Z_h$,

where $U_h \subset V^{d-1}$, $W_h \subset V$, and $Z_h \subset Y^{d-1}$ are some finite-dimensional subspaces. In order to do so we can use our weak formulation with one important modification. Since our approximation space does not guarantee continuity across the inter-element boundaries, the integrands in the boundary integrals have to be replaced by suitably chosen numerical fluxes preserving consistency and stability of the method. The semi-discrete finite element solution $(\mathbf{U}_{xy}(t,\cdot), \mathcal{Q}(t,\cdot))$ is obtained by requiring that for any $t \in [0,T]$, all $\Omega_e \in \mathcal{T}_h$, and for all $(\boldsymbol{\phi}, \Psi) \in U_h \times Z_h$ the following holds:

$$\int_{\Omega_e} \frac{\partial \mathbf{U}_{xy}}{\partial t}\ \boldsymbol{\phi}\ dxdydz + \int_{\partial\Omega_e} (\hat{\mathbf{C}}_{M,\mathbf{n}} + \sqrt{\mathcal{D}}\hat{\mathcal{Q}}\cdot\mathbf{n})\ \boldsymbol{\phi}\ ds \tag{25}$$
$$- \int_{\Omega_e} (\mathcal{C}_M + \sqrt{\mathcal{D}}\mathcal{Q})\cdot\nabla\boldsymbol{\phi}\ dxdydz = \int_{\Omega_e} \mathbf{F}\ \boldsymbol{\phi}\ dxdydz,$$
$$\int_{\Omega_e} \sqrt{\mathcal{D}^{-1}}\ \mathcal{Q}\ \Psi\ dxdydz = -\int_{\partial\Omega_e} \hat{\mathbf{U}}_{xy}\ \Psi\cdot\mathbf{n}\ ds \tag{26}$$
$$+ \int_{\Omega_e} \mathbf{U}_{xy}\ \nabla\cdot\ \Psi\ dxdydz, \tag{27}$$

where $\hat{\mathbf{C}}_{M,\mathbf{n}}$ is a solution to the Riemann problem for the nonlinear boundary flux $\mathcal{C}_M\cdot\mathbf{n}$. We set $\hat{\mathbf{U}}_{xy}$, $\hat{\mathcal{Q}}$ equal to the averages of the corresponding variables on both sides of the discontinuity. (Note, that there are other possible choices of $\hat{\mathbf{U}}_{xy}$ and $\hat{\mathcal{Q}}$.)

Discretization of the primitive continuity equation is done in a similar way. Let $\Omega_{e,xy}$ be the orthogonal projection of Ω_e into the xy-plane. We multiply (16) by a smooth test function $\delta = \delta(x,y)$, integrate it over $\Omega_{e,xy}$, and integrate by parts. Then, the mass balance in the water column corresponding to the 2D element $\Omega_{e,xy}$ can be expressed as

$$\int_{\Omega_{e,xy}} \frac{\partial h}{\partial t}\ \delta\ dxdy + \int_{\partial\Omega_{e,xy}} \mathbf{C}_{\mathbf{H}}\cdot\mathbf{n}\ \delta\ ds - \int_{\Omega_{e,xy}} \mathbf{C}_{\mathbf{H}}\cdot\nabla_{xy}\ \delta\ dxdy = 0, \tag{28}$$

Noting that $\mathbf{C}_{\mathbf{H}} = \left(\int_{z_b}^{\xi} u dz, \int_{z_b}^{\xi} v dz\right)^T$ and using the facts that δ is independent of z and that $h > 0$ we can transform the equation above as follows:

$$\int_{\Omega_{e,xy}} \frac{\partial h}{\partial t}\ \delta\ dxdy\ + \sum_{\Omega_e \in col(\Omega_{e,xy})} \int_{\partial\Omega_{e,lat}} \frac{\mathbf{u}_{xy}h\cdot\mathbf{n}}{h}\ \delta\ ds \tag{29}$$
$$- \sum_{\Omega_e \in col(\Omega_{e,xy})} \int_{\Omega_e} \frac{\mathbf{u}_{xy}h\cdot\nabla_{xy}}{h}\ \delta\ dxdydz = 0,$$

where $\partial\Omega_{e,lat}$ denotes the lateral boundary faces of prism Ω_e, and $col(\Omega_{e,xy})$ is the set of 3D elements in the water column corresponding to $\Omega_{e,xy}$. Note, that the expression above is well defined for any $\delta(x,y) \in \mathcal{H} \stackrel{\text{def}}{=} L^2(\Omega_{xy}) \bigcap \{h : h_{|\Omega_{e,xy}} \in H^1(\Omega_{e,xy}), \forall \Omega_e \in \mathcal{T}_h\}$ and $h(t,x,y) \in H^1(0,T;\mathcal{H})$, where Ω_{xy} is the orthogonal projection of the domain Ω into the xy-plane.

Analogous to the momentum conservation equations, we seek an approximation $H(t,\cdot) \in \mathcal{H}_h$ to the solution of the weak problem $H(t,\cdot)$, where $\mathcal{H}_h \subset \mathcal{H}$ is some finite dimensional subspace. Using the weak formulation, (29) and replacing integrands in the boundary integrals by a suitable numerical flux, we obtain our semi-discrete finite element solution $H(t,\cdot) \in \mathcal{H}_h$ by requiring that for any $t \in [0,T]$, all $\Omega_e \in \mathcal{T}_h$, and for all $\delta \in \mathcal{H}_h$ the following holds:

$$\int_{\Omega_{e,xy}} \frac{\partial H}{\partial t}\ \delta\ dxdy\ + \sum_{\Omega_e \in col(\Omega_{e,xy})} \int_{\partial\Omega_{e,lat}} \frac{\hat{C}_H}{\xi_s - z_b}\ \delta\ ds \qquad (30)$$
$$- \sum_{\Omega_e \in col(\Omega_{e,xy})} \int_{\Omega_e} \frac{\mathbf{U}_{xy} H \cdot \nabla_{xy}}{\xi_s - z_b}\ \delta\ dxdydz = 0.$$

Here $\hat{C}_H$ is a solution to the Riemann problem for the normal boundary flux $\mathbf{U}_{xy} H \cdot \mathbf{n}$, and ξ_s denotes the value of the z coordinate at the free surface of the smoothed mesh. This boundary flux formulation has several important advantages. It transforms integrals over 2D edges into integrals over lateral faces of 3D elements, thus allowing us to solve the Riemann problem for elevation simultaneously with the corresponding problem for the momentum equations; it is consistent with the continuous formulation; and it takes into account the coupling between velocity and elevation which is crucial for stability of our numerical scheme.

Finally, we turn to the space discretization for continuity equation (3). Unlike the mass and momentum conservation equations it is not time-dependent, its main role being computation of the vertical velocity component w to maintain a divergence-free velocity field. Regarding the continuity equation with the boundary condition at the bottom as an initial value problem for w, we can solve it element by element in each water column starting at the bottom and using the solution from the element below to provide an initial condition.

Multiplying (3) by a smooth test function σ, integrating it over Ω_e, integrating by parts, and re-ordering terms we obtain a weak formulation (recall

that $n_z = 0$ on the lateral faces):

$$\int_{\partial\Omega_{e,top}} w\ n_z\ \sigma\ ds - \int_{\Omega_e} w \left(\frac{\partial\sigma}{\partial z}\right) dxdydz = \tag{31}$$
$$\int_{\Omega_e} \mathbf{u}_{xy} \cdot \nabla_{xy}\sigma\ dxdydz - \int_{\partial\Omega_{e,bot}} w\ n_z\ \sigma\ ds - \int_{\partial\Omega_e} \mathbf{u}_{xy} \cdot \mathbf{n}\ \sigma\ ds,$$

where $\partial\Omega_{e,top}, \partial\Omega_{e,bot}$ denote the top and bottom boundaries of element Ω_e.

We seek $W(t,\cdot) \in W_h$, where W_h is some finite dimensional subspace of V, such that for given values of $\mathbf{U}_{xy}(t,\cdot) \in U_h$, for all $\Omega_e \in \mathcal{T}_h$, and for all $\sigma \in W_h$ the following holds:

$$\int_{\partial\Omega_{e,top}} W\ n_z\ \sigma\ ds - \int_{\Omega_e} W \left(\frac{\partial\sigma}{\partial z}\right) dxdydz = \tag{32}$$
$$\int_{\Omega_e} \mathbf{U}_{xy} \cdot \nabla_{xy}\sigma\ dxdydz - \int_{\partial\Omega_{e,bot}} W^-\ n_z\ \sigma\ ds - \int_{\partial\Omega_e} \hat{C}_w\ \sigma\ ds,$$

where W^- is an initial value for W taken from the element below (or a boundary condition at the bottom in the case of the bottommost element), and $\hat{C}_w$ is a numerical flux for the normal boundary flux function $\mathbf{U}_{xy} \cdot \mathbf{n}$. On the lateral boundaries $\hat{C}_w$ should be set equal to $\frac{\hat{C}_H}{\xi_s - z_b}$ (comp. with (30)) in order to preserve the local mass conservation properties of our numerical scheme. On horizontal faces it can be taken equal to the average or upwinded value of the corresponding variables.

5 A shock detection algorithm for the discontinuous Galerkin method

In this section, we will give a brief description of the shock detection algorithm for discontinuous Galerkin methods developed by Krivodonova and Flaherty with various collaborators. For details, see [3] and references therein. This shock detection technique is based on superconvergence results for the discontinuous Galerkin method for conservation laws [1].

Let $\mathcal{T}_{\Delta x}$ be a partition of a 2- or 3D domain Ω, and let $\Omega_e \in \mathcal{T}_{\Delta x}$. We denote by $\partial\Omega_e^i$, $\partial\Omega_e^o$ the inflow ($\mathbf{u} \cdot \mathbf{n}_e < 0$) and the outflow ($\mathbf{u} \cdot \mathbf{n}_e \geq 0$) boundaries of Ω_e, where $\mathbf{u}$ is the flow velocity vector, and $\mathbf{n}_e$ is a unit exterior normal to $\partial\Omega_e$. Let y be a state variable in our system. If y is smooth,

then $Y_e \in P^k(\Omega_e)$, the DG approximation for y on Ω_e, has the following superconvergence properties for $k \geq 0$:

$$\frac{1}{|\partial\Omega_e^o|}\int_{\partial\Omega_e^o}(Y_e - y)\,ds \;=\; O\left(\Delta x_e^{2k+1}\right), \tag{33}$$

where $|\partial\Omega_e^o|$ is the measure of $\partial\Omega_e^o$.

This property of the DG solution can be exploited to construct a shock-detector. We define

$$\mathcal{I}_e \;= S\,\frac{\left|\int_{\partial\Omega_e^i}[Y]ds\right|}{\Delta x_e^{(k+1)/2}\,|\partial\Omega_e^i|}, \tag{34}$$

where $[Y]$ denotes the jump in the DG solution Y over the element boundary, Δx_e is the diameter of element Ω_e, and S is a scaling parameter that can be taken as $S = \|Y\|^{-1}_{L^\infty(\Omega_e)}$ for Δx_e small enough and Y bounded away from zero. For $\mathcal{I}_e$ defined as above, we have $\mathcal{I}_e \to 0$ as $\Delta x_e \to 0$ in smooth solution regions whereas $\mathcal{I}_e \to \infty$ as $\Delta x_e \to 0$ if y is discontinuous.

6 Numerical Results

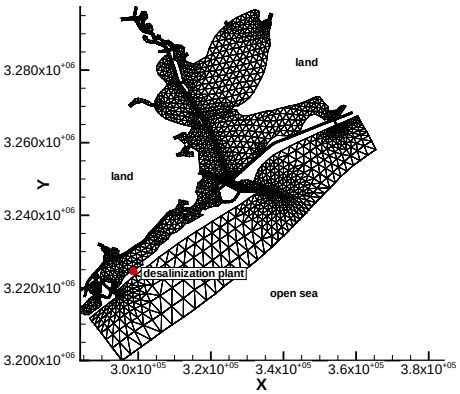

Figure 1: Galveston Bay finite element mesh. Lengths are in meters.

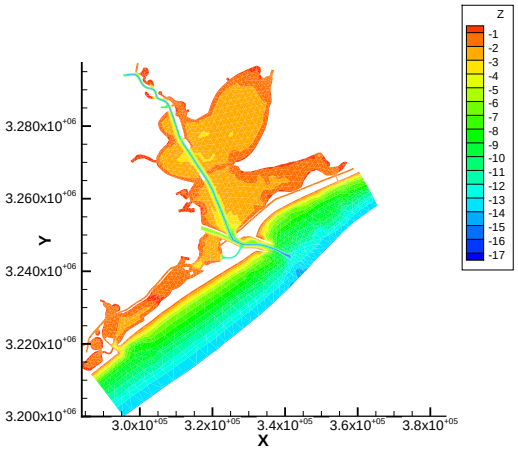

Figure 2: Galveston Bay bathymetry. Lengths are in meters.

We conclude this report with a numerical example demonstrating capabilities of UTBEST-3D when applied to baroclinic problems.

Here, we consider a desalinization plant injecting water with a high concentration of salt into bay. The salinity of the bay water is set to 35ppt, the plant outflow is taken to be 10 m^3/s at 70ppt. The simulation was started cold (zero surface elevation and velocity), and the following tidal forcing was imposed on the open sea boundaries:

$$\begin{aligned}\hat{\xi}(t) &= 0.075\cos(\tfrac{t}{25.82}+3.40) + 0.095\cos(\tfrac{t}{23.94}+3.60) \\ &+ 0.100\cos(\tfrac{t}{12.66}+5.93) + 0.395\cos(\tfrac{t}{12.42}+0.00) \\ &+ 0.060\cos(\tfrac{t}{12.00}+0.75) \quad (meters).\end{aligned} \tag{35}$$

In all runs, the time stepping was performed using explicit TVD Runge-Kutta schemes described in [2] of the order matching the order of the space discretization. The Riemann problems on the lateral boundary faces were handled by Roe's solver and those on horizontal faces by an upwind flux. The initial 2D mesh and bathymetry are shown in Figures 1, 2. In the vertical direction, the mesh was subdivided in up to five equidistant layers.

The problem was solved using piecewise linear approximation spaces with one layer of adaptive mesh refinement. In Figure 3 we plot the salinity plume in the vicinity of the desalinization plant outflow site for days 1-5.

References

[1] S. Adjerid, K. D. Devine, J. E. Flaherty, L. Krivodonova, *A posteriori error estimation for discontinuous Galerkin solutions of hyperbolic problems*, Computer Methods in Applied Mechanics and Engineering, 191, pp. 1097-1112, 2002.

[2] B. Cockburn and C.-W. Shu, *TVB Runge-Kutta local projection discontinuous Galerkin finite element method for scalar conservation laws II: General framework*, Math. Comp., 52, pp. 411-435, 1989.

[3] L. Krivodonova, J. Xin, J.-F. Remacle, N. Chevaugeon, J.E. Flaherty, *Shock Detection and Limiting with Discontinuous Galerkin Methods for Hyperbolic Conservation Laws*, Applied Numerical Mathematics, to appear.

[4] R.A. Luettich, J.J. Westerink, N.W. Scheffner, *ADCIRC: An Advanced Three-Dimensional Circulation Model for Shelves, Coasts and Estuaries,* Report 1, U.S. Army Corps of Engineers, Washington, D.C. 20314-1000, December 1991.

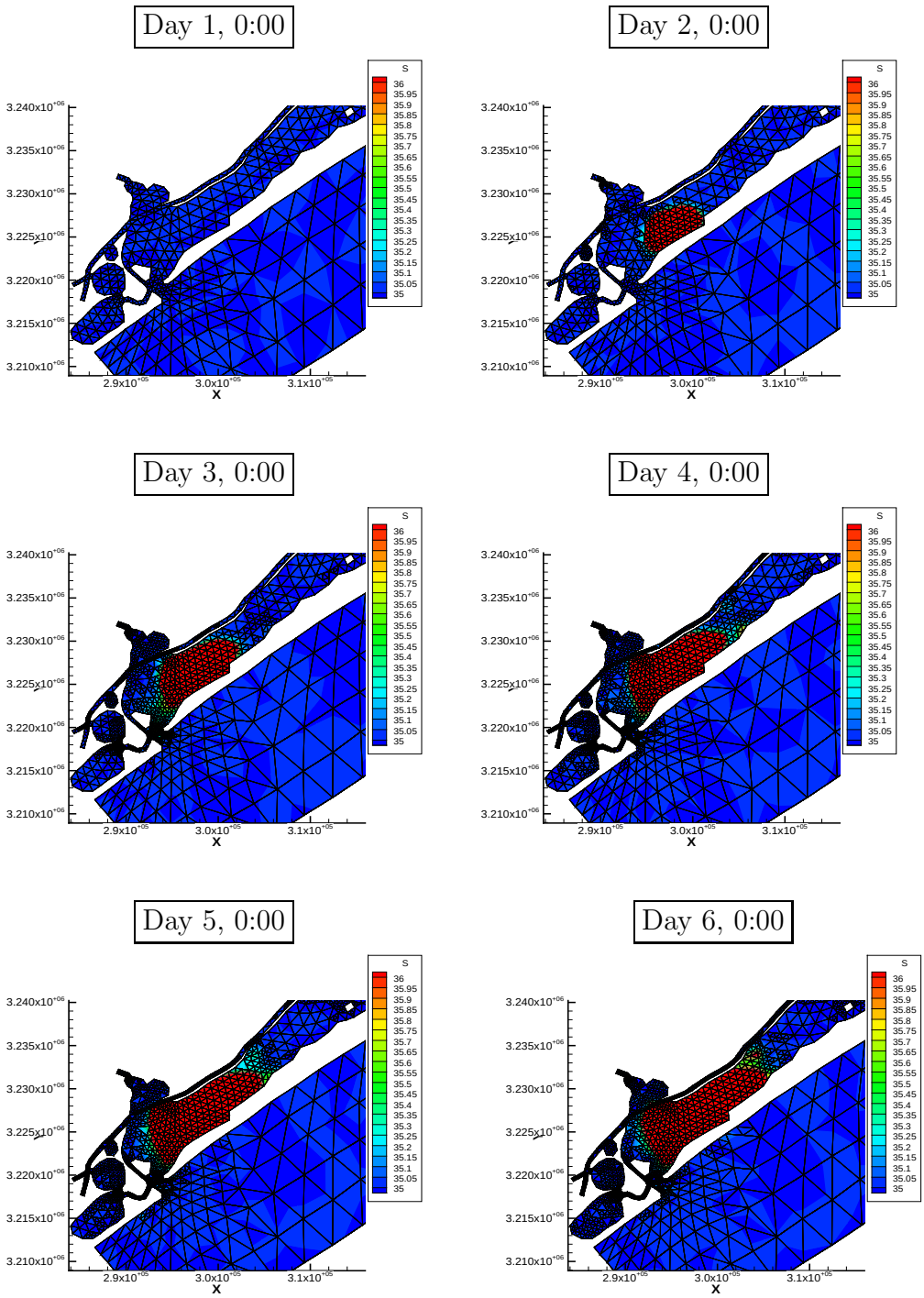

Figure 3: Desalinization plant outflow simulation. Lengths are in meters.